

Removal of residual chromium from aluminum oxide by containerless liquid-phase processing

A. Biswas, Microgravity Research Group, Jet Propulsion Laboratory, California Institute of Technology, 4800 Oak Grove Drive, Pasadena, CA 91109.

J. K. Richard Weber and Paul C. Nordine, Container-less Research Inc., 910 University Place, Evanston, IL 60201,

ABSTRACT

Verneuil sapphire was purified of Cr^{3+} by containerless melting and processing at ca. 2550 K in high purity argon, dry air and pure oxygen. Recovered material was examined by laser induced fluorescence and Raman spectroscopy. The Cr^{3+} fluorescence intensity decreased in processed specimens at rates proportional to the chromium concentration and $p(\text{O}_2)^{0.21}$. The initial chromium concentration was ca. 5 ppm and decreased by factors of ca. 50, 3000 and 2×10^5 after processing for 300 seconds in argon, air and oxygen, respectively. Evidence is presented that the Cr^{3+} was removed predominantly as $\text{CrO}_2(\text{g})$ and not by conversion to other oxidation states of chromium in the condensed phase. A comparison of the Raman peak shifts for as-received and processed samples indicates that considerable stress was retained during containerless solidification of the highly undercooled melts.

1. INTRODUCTION

High purity aluminum oxide (sapphire) is widely used as an optical and laser host material. Metallic ion impurities, either deliberately added as dopants, or present as residual impurities, strongly influence the optical properties of the solid and the melt [1-4]. Cr^{3+} plays a prominent role in this regard. For example, the strong optical absorption of ruby peaked in the violet (~400 nm) and green (~543 nm) [5] regions of the visible spectrum, result from the addition of ~500 ppm of Cr^{3+} in the host sapphire. This absorbed radiation is responsible for exciting strong red fluorescent emission peaked at 694.3 nm and also known as the “R lines”. This emission forms the basis for operation of the ruby laser [6]. High purity **undoped** sapphire contains residual (~1-5 ppm) of Cr^{3+} as impurity. Even in such low concentrations, residual Cr^{3+} causes “ruby-like” absorption-fluorescence behavior. While the fluorescence in this case is much reduced compared to ruby it still gives rise to a strong signal [7,8] especially when excited by green laser light.

In principle, the high volatility of chromium oxides, $\text{CrO}_3(\text{g})$, $\text{CrO}_2(\text{g})$ and $\text{CrO}(\text{g})$ provides a means by which the chromium content of alumina can be reduced to exceedingly low values. For example, thermodynamic data [9] show that the activity of $\text{Cr}_2\text{O}_3 = 4.7 \times 10^{-7}$ in liquid **alumina**, when the total pressure of aluminum- and chromium- bearing species are equal, at an ambient oxygen pressure of 1 bar and a temperature of 2600 K. The gas phase **Cr:Al** concentration thus exceeds the condensed phase **Cr:Al** ratio by a large factor, and only a small loss of alumina would be required to greatly reduce the chromium impurity content by vaporization processes. This approach is similar to that used to remove oxide impurities from liquid metals by vaporization of suboxides under **containerless** conditions [10,11].

In the present work the removal of residual chromium from **Verneuil** sapphire was investigated by liquid-phase processing under the unique **containerless** conditions achieved

in an **aero-acoustic** levitator (AAL) [12]. Rapid stirring and diffusion in the liquid phase allowed bulk purification and temperatures up to 2650 K were achieved to enable rapid vaporization. The **containerless** processing method [12-14] used in this work **prevented** the severe contamination that would otherwise occur from container walls. Thus levitated molten samples **were** processed for varying lengths of time in argon, air and pure oxygen and these samples were subsequently subjected to laser induced fluorescence (**LIF**) measurements. The strength of the **R** line emission was used to determine the relative **Cr³⁺** concentrations in **the** starting and processed materials. **Raman** measurements [15,16] on these samples were also performed.

II. EXPERIMENTAL

Verneuil sapphire spheres (**Imetra, Inc., Elmsford, NY**) 0.3 cm in diameter and weighing approximately 55 mg were levitated at atmospheric pressure in jets of high purity argon, dry air, and pure oxygen using the AAL method [12]. Levitated material was melted by heating from two sides with **cw** CO₂ laser beams. Progress of the levitation experiments was monitored with video cameras. The time at which the specimen melted was determined from the video image by observing the shape change which accompanied melting. The specimen temperature was **measured** continuously with an automatic optical pyrometer whose operating wavelength was 0.65 micrometers, The specimen temperature was also measured periodical] y with a manual optical pyrometer (Micro-Optical Pyrometer, Pyrometer Instrument Company, **Northvale, NJ**). The experiments were similar to those conducted in prior studies that used **aero-acoustic** levitation to process liquid aluminum oxide under **containerless** conditions [12-14], A detailed description of the levitator is presented in reference [12].

The molten specimens were held at temperatures in the range 2500-2600 K for periods of 30, 60, 120, 180 and 300 seconds and then cooled to ambient temperature under

container-less conditions by blocking the heating laser beam. The processing time was recorded as the interval between melting and x-e-solidification of the specimen as observed via the video cameras and the optical pyrometer,

Figure 1 illustrates the apparatus for Raman scattering and laser induced fluorescence measurements on the processed samples. Light scattered normal to the 514.5 nm argon laser propagation direction was collected and focused on to the double monochromator. The wavelength dependent signal was sensed by a photomultiplier tube (PMT). The PMT signal after amplification was fed to the photon counter and the recorded counts were subsequently stored in a computer.

The as-received samples were smooth, transparent, single crystalline spheres with a Cr^{3+} concentration estimated to be ca. 5 ppm [17]. The microstructure and scattering characteristics of the processed samples were different from the as-received spheres and were also dependent on process conditions [14]. The intensity of incident laser radiation and that of collected LIF and Raman signals depended on the sample scattering characteristics. In order to account for different scattering in the processed and as-received samples, the Raman and LIF results were obtained with the same experimental set-up. Chromium removal was then determined from the ratios of the measured LIF and Raman intensities. Slight differences in optical alignment caused some scatter in the results, but this scatter was small compared with the large changes in the LIF:Raman intensity ratios that resulted from changes in the Cr^{3+} concentrations.

111. RESULTS

This section summarizes the observations during liquid phase processing experiments and the results of the LIF and Raman measurements.

Liquid Phase Processing Experiments:

Specimens were easily levitated and melted. Melting was achieved more rapidly in argon than in oxygen and required 10-15 seconds upon exposure of the levitated sample to the heating CO₂ laser beam. Molten specimens were held at temperatures of 2500 to 2600 K for 30-3000 seconds. Temperature differences of approximately 50 K were observed between the hotter, laser heated regions at the sides of the molten specimens and the cooler bottom and top parts.

All of the liquid specimens cooled to a temperature 350-450 K below the equilibrium melting temperature when the heating beam was blocked. The undercooling was followed by rapid solidification. Release of the heat of fusion resulted in a temperature rise to the melting point at which complete solidification occurred and then the specimen cooled to ambient temperature.

Mass losses during processing were 0.06 to 0.64 mg. The mass losses were the result of slight spalling or liquid fragmentation during the melting of some specimens and did not correlate with the duration of processing.

LIF and Raman Measurements:

Table 1 presents the results of the spectroscopic measurements. Figure 2a and 2b show typical spectra obtained in the fluorescent emission and Raman scattering regions, respectively.

The intensities of the Raman peak at ~418 cm⁻¹ given in Table 1 were used to normalize the LIF measurements. The normalized intensities proportional to the LIF:Raman intensity

ratio, are also given in Table 1. Figure 3 presents a semi-log plot of these normalized LIF intensities as a function of processing time t . Least squares fits of the data, constrained to have equal intercepts, are given by the straight lines drawn through the data. The least squares fits are given by the following equations:

Argon: $\text{Log}(I) = -0.0048 t + 5.93$

Air: $\text{Log}(I) = -0.0112 t + 5.93$

Oxygen: $\text{Log}(I) = -0.0156 t + 5.93$

The initial Cr^{3+} concentration in the material was estimated to be 5 ppm [17]. The results indicate that the residual Cr^{3+} concentration of 5×10^{-6} decreased after processing for 300 seconds to 1×10^{-7} in argon, 1.7×10^{-9} in air and 2×10^{-11} in oxygen. The rates of Cr^{3+} removal, as represented by the slopes in Figure 3 are larger in oxygen than in air or argon. The mole fraction of oxygen in air is 0.208, and the slope in air is 0.72 of that in oxygen. These results indicate that the rate of Cr^{3+} removal is proportional to the 0.21 \pm 0.05 power of the ambient oxygen partial pressure.

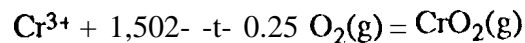
IV. DISCUSSION

The processed samples were formed by rapid solidification from the undercooled melts. The melts were initially undercooled by 350- 450°C, at which temperatures 60 to 80% of the melt would be consumed in adiabatic solidification to form a liquid-solid mixture at the melting point. This initial solidification process occurred in a few milliseconds. It was followed by solidification of the remaining melt in approximately 1 second due to further heat loss, and rapid cooling of the solid to ambient temperature. These processing conditions are likely to produce residual stress in the solid materials formed. In all cases

the Raman peak shifts given in Table 1 for the processed samples exceed the mean value for as-received single crystal sapphire samples. This difference of a sign and magnitude comparable to the stress dependent Raman shifts reported [16] for loaded sapphire filaments, In view of the rapid processing conditions, we suggest that the Raman peak shifts found here are also due to stresses in the processed samples.

The reduction in Cr^{3+} concentration measured by LIF experiments might be attributed to a change in the oxidation state rather than the loss of residual chromium contained in the processed specimens. However, such a change would have to be to a higher oxidation state to be consistent with the greater rates of removal in oxygen than in argon, and would not lead to a continued linear change of the Cr^{3+} concentration with time. Moreover the removal would occur more rapidly than the rate observed. In other research [18], we have demonstrated that equilibration of liquid aluminum oxide with oxygen or argon occurs in a few seconds to cause a distinct change in the spectral absorption coefficient of the liquid. Also, the terminal solid at high temperatures in the Cr-O phase diagram [19] is Cr_2O_3 , even though higher oxides of chromium can be formed at low temperatures.

The reaction kinetics are also consistent with the conclusion that the chromium content is present as Cr^{3+} whose concentration is controlled by a gasification process. Thermodynamic data [14] show that the significant chromium-bearing gaseous species under all processing conditions are $\text{CrO}(\text{g})$, $\text{CrO}_2(\text{g})$ and $\text{CrO}_3(\text{g})$ in proportions of approximate] y 0.13:1,0:0.31 at 2600 K. Since CrO_2 is the major species, we take the vaporization reaction to be:



The concentration of oxygen ions in the host aluminum oxide is independent of the chromium concentration and the pressure of $\text{CrO}_2(\text{g})$ resulting from this reaction will be

proportional to $p(\text{O}_2)^{0.25}$. Corrections for the equilibrium $\text{CrO}:\text{CrO}_2:\text{CrO}_3$ ratios that occur will change this dependence slightly, resulting in a rate which is proportional to $p(\text{O}_2)^{0.268}$. This $p(\text{O}_2)$ dependence agrees with the 0.21 ± 0.05 value derived from the rate data in oxygen and air. The postulated reaction also provides the required first-order process. Assuming the measured $p(\text{O}_2)^{0.21}$ dependence, a partial pressure of oxygen equal to 3.8×10^{-3} is derived for the experiments in argon. This small value is qualitatively consistent with the degree of mixing of air into the levitation gas jet that has been observed via oxidation of levitated metal specimens [12].

V. CONCLUSION

This work demonstrated the application of containerless liquid-phase processing to remove chromium from liquid aluminum oxide. The high sensitivity of laser fluorescence detection of Cr^{3+} allowed detection of extremely small Cr^{3+} concentrations. A high purity equal to a few parts in 10^{11} of Cr^{3+} in aluminum oxide was achieved by processing in oxygen. The Raman peak shift of the 418 cm^{-1} line in the as-received and processed samples indicate that considerable stress was retained during containerless solidification of the highly undercooked melts.

ACKNOWLEDGMENT

Support for the performance of this research was provided at the Jet Propulsion laboratory, California Institute of Technology, under contract to the National Aerospace and Aeronautics Administration. At CRJ Inc. this work was supported by NASA Microgravity Science and Applications Division under Grant Number NASW-4688. Part of the cost of the Aero-Acoustic Levitation was supported by NSF under grant Number IS1-906-1 168.

REFERENCES

1. D. L. Parry and M. Q. Brewster, "Propellant Al_2O_3 Particle Size and Optical Constants from *in-situ* Light Scattering and Extinction Measurements", *J. Thermophys. and Heat Transfer*, S, 142-49 (1991).
2. D. S. McClure, "Optical spectra of Transition-Metal Ions in Corundum, *J. Chem. Phys.*, 36, 2757, (1962).
3. R. A. Reed, V. S. Calia, J. K. R. Weber, S. Krishnan, P. C. Nordine, C. D. Anderson and M. McKee, "New Measurements and Modelling of Liquid Aluminum Oxide", *Proc. JANAF Exhaust Plume Technology Mtg.*, 9-11 Feb. 1993, Albuquerque, NM, CPIA (in Press).
4. J. K. R. Weber, S. Krishnan, C. D. Anderson and P. C. Nordine, "Spectral Absorption Coefficient of Liquid Aluminium Oxide from 0.42-0.78 μm " *J. Am. Ceram. Soc.* (In Press).
5. D. C. Cronmeyer, "Optical Absorption Characteristics of Pink Ruby", *Journal of the Optical Society of America*, 56, 1703, (1966).
6. P. W. Milonni, J. H. Eberly, *Lasers* (John Wiley & Sons Inc., 1988), pp. 412-414.
7. D. Lapraz, P. Iacconi, D. Daviller and B. Guilhot, "Thermally Stimulated Luminescence and Fluorescence of $\alpha\text{-Al}_2\text{O}_3\text{:Cr}^{3+}$ Samples (Ruby)", *Physics Status Solidi*, 126, 521, (1991),

8. H. Liu, K. S. Lim, W. Jia, E. Strauss, W. M. Yen, A.M. Buoncristiani, and C. E. Byvik, " Effects of Tensile Stress on the R Lines of Cr³⁺ in a Sapphire Fibre", *Optics Letters*, 13,931, (1988).
9. M. W. Chase Jr., C. A. Davies, J. R. Downey Jr., D. J. Frurip, R. A. Macdonald and A. H. S yverud, (*JANAF Thermochemical Tables*, J. Phys. Chem. Ref. Data, 1985) 3rd Edition, pp. 14.
10. I... Brewer and G.M. Rosenblatt , "Thermodynamics of Suboxide Vaporization", *Trans. Met. Sot. AIME*, 224, 1268, (1962).
11. S. Krishnan, J. K. R. Weber, P. C. Nordine, R. A. Schiffman, R. Hauge and J. L. Margrave, "Spectral Emissivities and Optical Properties of Liquid Silicon, Aluminum, Titanium and Niobium at 632.8 nm", *High Temperature Science*, 30, 137, (1991).
12. J. K. R. Weber, D. S. Hampton, D. R. Merkeley, C. A. Rey, M. M. Zatarski and P. C. Nordine, "Aero-Acoustic Levitation - A Method for Containerless Liquid Phase Processing at High temperatures", *Rev. Sci. Instrum.*, 65, 1, (1994).
13. J. K. R. Weber, S. Krishnan, and P. C. Nordine "The Use Of Containerless Processing in Researching Reactive Materials", *J, Metals*, 43, 8, (1991).
14. J. K. R. Weber, C. D. Anderson, S. Krishnan, and P. C. Nordine, "Structure of Aluminum Oxide Formed from Undercooked Melts", *J. Am. Ceram. Sot.* (In Press).
15. S. P. S. Porto, and R. S. Krishnan, "Raman Effect of Corundum", *J, Chem. Phys.* 47, 1009, (1967)

16. W. Jia and W. M. Yen, "Raman Scattering from Sapphire Fibers", *J. Raman Spectroscopy*, 26,785, (1989).
17. Andre Deglon, Denimex Development, private communication.
18. J. K.R. Weber, P. C. Nordine and S. Krishnan, "Effects of Melt Chemistry on the Spectral Absorption Coefficient of Molten Aluminum Oxide", *J. Am. Ceram.Soc.*, (submitted).
19. T. B. Massalski, J. L. Murray, L. H. Bennett, H. Baker, and L. Kacprzak, eds. *Binary Alloy Phase Diagrams, Vol. 1* (ASM, Metals Park, Ohio, 1986) pp. 845-846.

Table I. Showing the LIF and Raman Peak positions and intensities

Sample Type	Processing Time (secs.)	Raman Peak (cm ⁻¹)	Raman Intensity (cps)	LIF Peak (cm ⁻¹)	LIF Intensity (cps)	Normalized LIF Intensity
<i>As-reed</i>	0	418.13	114	5033.60	179054	849721
Air	30	418.95	368	5033.20	117162	172241
Air	60	418.80	497	5032.78	138344	150592
Air	120	419.19	541	5033.06	34190	34190
Air	180	418.55	480	5032.30	6703	7555
Air	300	419.81	405	5032.3	1031	1377
Oxygen	30	419.11	403	5034.13	183571	246432
oxygen	60	419.68	298	5033.10	6629	12035
Oxygen	120	418.87	387	5033.60	4375	6116
Oxygen	180	418.30	328	5034.11	2814	4641
Oxygen	300	418.95	514	5033.60	41	43
Argon	30	418.87	400	5034.13	251785	340539
Argon	60	419.84	507	5033.98	401786	428730
Argon	120	419.11	442	5032.70	202678	248074
Argon	180	419.11	435	5034.12	195000	242517
Argon	300	418.30	355	5034.13	12054	18370

LIST OF FIGURES

Figure 1 Showing a schematic arrangement for **LIF** and **Raman** measurements of the **as-received** sapphire and processed samples.

Figure 2 (a) Typical **LIF** spectra obtained from the as-received sapphire samples and (b) representative Raman spectra of the same. The peak at $\sim 418\text{ cm}^{-1}$ was used to normalize the LIF intensity.

Figure 3 Log normalized **LIF** intensity versus time plots for samples processed in argon, air and oxygen. The lines represent best fits to the data obtained by constraining the intercept.

